ELSEVIER

Journal of Photochemistry and Photobiology A: Chemistry 138 (2001) 185–192

Journal of Photochemistry and Photobiology A:Chemistry

www.elsevier.nl/locate/jphotochem

Comparative assessment of the efficiency of TiO_2/OTE thin film electrodes fabricated by three deposition methods Photoelectrochemical degradation of the DBS anionic surfactant

H. Hidaka [a,*], K. Ajisaka [a], S. Horikoshi [a], T. Oyama [b], K. Takeuchi [b], J. Zhao [c], N. Serpone [d]

[a] *Frontier Research Center for the Global Environment Protection, Meisei University, 2-1-1 Hodokubo, Hino, Tokyo 191-8506, Japan*
[b] *The Institute of Physical and Chemical Research, Hirosawa, Wako, Saitama 351-0198, Japan*
[c] *Institute of Photographic Chemistry, Chinese Academy of Sciences, Beishatan, Beijing 100101, China*
[d] *Department of Chemistry and Biochemistry, Concordia University, Montreal, Que., Canada H3G 1M8*

Received 23 March 2000; received in revised form 31 July 2000; accepted 3 October 2000

Abstract

This study reports on a comparative assessment of the efficiencies of TiO_2/SnO_2-doped OTE thin film electrodes fabricated by three different deposition methods. Process efficiencies, as measured by the kinetics of degradation, were examined by monitoring the photo-oxidative fate of two test substrates, namely the anionic surfactant sodium dodecylbenzenesulfonate (DBS) and the model compound sodium benzenesulfonate (BS). Methods chosen to fabricate the TiO_2/OTE electrodes comprised (i) pulsed laser deposition, (ii) deposition of a TiO_2 paste on the OTE plate, and (iii) sol–gel deposition. Both DBS and BS are readily photo-oxidized and, under our conditions, were partially mineralized to CO_2 with the process being made particularly more efficient when the TiO_2/OTE electrodes were anodically biased at +0.3 V, which generated a photocurrent during the photoelectrolysis. The sol–gel {C} and anatase {B1} electrodes proved especially useful under the +0.3 V bias. In the absence of any bias, however, DBS photodegraded faster on the TiO_2-pasted electrode. Under otherwise similar conditions, the pulsed laser rutile TiO_2/OTE electrode showed very little photoactivity. Some of the characteristics of the TiO_2 film, such as the TiO_2 crystalline form, film thickness, surface roughness, and film transparency appear to have some effect on the overall photodegradative process efficiency.

Keywords: TiO_2/OTE thin film; DBS anionic surfactant; Photoelectrochemical degradation

1. Introduction

Environmentally polluted waters and air pose serious global concerns. Such alternative technologies as advanced oxidation processes (AOP) are being actively considered to abate the growing environmental pollution. A promising technique is the photocatalytic degradation process that has hitherto involved mostly TiO_2 semiconductor particulates. Ever since the first paper on the photocatalyzed oxidation of tetralin over TiO_2 by Kato and Mashio in the mid-1960s [1], identification of intermediates and final oxidation products, and in some cases process pathways, TiO_2 aqueous dispersions have been examined extensively from both an applied and fundamental points of view. Unfortunately, for practical applications TiO_2 particulates impart some disadvantages as they have to be removed either by centrifugation and/or by filtration after the photo-oxidation of the polluted feed. By contrast, a TiO_2-fixed system needs no such batch operation and continuous wastewater treatments become more practical.

The degradation of chlorinated compounds [2,3] and dyes [4,5] have been examined photoelectrochemically on TiO_2-coated glass electrodes. Irradiation of the TiO_2 thin film leads to the photogeneration of electrons and holes; application of an anodic bias of +0.3 V causes the electrons in the TiO_2 film to migrate to an external circuit, thereby suppressing electron/hole recombination and allowing the holes to accumulate at the film surface as trapped holes (i.e. $^{\bullet}OH_{surf}$ radicals) poised to initiate photo-oxidative degradation of adsorbed substrates (see Scheme 1).

Aromatic compounds [6] and formic acid [7,8] have also been photodegraded on TiO_2 thin film electrodes prepared either by the sol–gel [9,10] or by the Ti-firing technique [11]. A pasted TiO_2 thin film electrode was used to degrade surfactants [12], organic acids [13], and amino acids [14]. However, none of the above studies addressed in a systematic and significant way which type of electrode, and

* Corresponding author.
E-mail address: hidaka@epfc.meisei-u.ac.jp (H. Hidaka).

1010-6030/01/$ – see front matter
PII: S1010-6030(00)00389-0

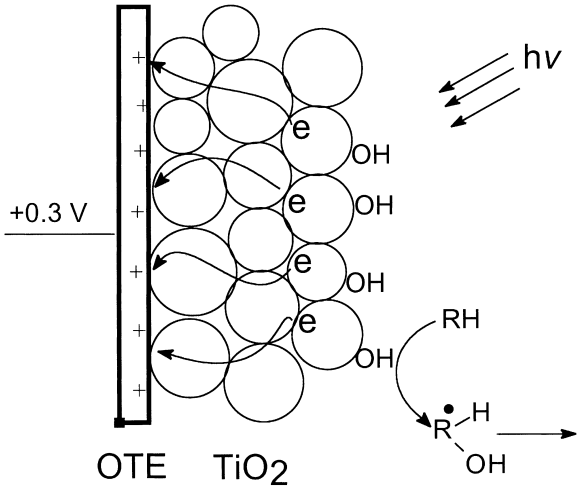

Scheme 1.

thus which fabrication procedure might be most useful and photo-oxidatively most efficient toward degradation of some given feed.

The present study examines the photodecomposition of two organic pollutants, namely the anionic surfactant sodium dodecylbenzenesulfonate (DBS) and the model compound sodium benzenesulfonate (BS), to assess which of the three procedures might yield the more efficient TiO_2/OTE electrode(s) with and without external bias. The three fabrication methods were (i) the pulsed laser method, (ii) the TiO_2 pasting procedure, and (iii) the sol–gel coating method. As an added benefit, a photocurrent was generated during the course of the photoelectrochemical degradation of the pollutants. The surfaces of the TiO_2 films were characterized by scanning electron microscopy (SEM) and by X-ray diffraction techniques (XRD). The photoelectrochemical degradations of DBS and BS were monitored by the disappearance of the aromatic ring (absorption in the UV region) and by CO_2 evolution using gas chromatography.

2. Experimental

2.1. Preparation of TiO_2/OTE electrodes

Optically transparent electrodes (OTEs) of SnO_2/sodalime glass (sheet resistance, 5.6 Ω/cm^2; thickness of SnO_2 film, 960 nm; haze, 14%; transparency, 83.5%; dimensions of the OTE plate, 20 mm × 40 mm) were a gift from the Asahi Glass Co. An area of 20 mm × 30 mm of the OTE plate was used to coat with TiO_2; the remaining portion (20 mm × 10 mm) was left naked to permit suitable electrical connection of the electrode to the external circuit. Three different procedures were favored to fabricate the TiO_2/OTE electrodes denoted below as {A}, {B}, and {C}.

{A} A TiO_2/OTE electrode (pasting method) was prepared by addition of 100 mg of TiO_2 particles (Degussa P-25; particle size ca. 33 nm, particle surface area ca. 55 m^2/g) to 50 ml of deionized water to yield a TiO_2/H_2O suspension that was ultrasonicated for 5 min and then pasted onto the OTE plate. The plate was subsequently dried and the TiO_2 film particulates sintered at 300°C for 1 h in an electric furnace. Two electrodes were assembled by this method differing in the loading of TiO_2 on the OTE plate.

{B} To prepare the electrode by the pulsed laser deposition method [15], an OTE plate was positioned inside a 3-l spherical glass photoreactor appropriately modified to have a quartz window as the inlet for the laser pulse. A reactant mixture of $TiCl_4$, H_2 and O_2 gases in various ratios was introduced into the glass reactor, following which the mixture was irradiated with a Nd-YAG laser pulse (wavelength, 1064 nm; pulse energy, 1 J; pulse width, 10 ns) focused in the center of the reactor with a 200-mm (focal length) lens. The overall reaction occurred in many steps: (i) reaction of H_2 with O_2 to form •OH radicals and H_2O, and (ii) hydrolysis of $TiCl_4$ by the •OH radicals and/or H_2O to yield TiO_2 particles (anatase and/or rutile) which deposited on the plate. The TiO_2 crystalline type depended on the mole ratio of $TiCl_4$, H_2 and O_2 gases introduced which affords a means to control the anatase/rutile TiO_2 ratio. Only rutile formed in a large excess of H_2. By contrast, exclusive formation of anatase occurred when equal amounts of H_2 and O_2 were used. Mixtures of anatase and rutile fine particles were obtained in the presence of excess O_2. The TiO_2-deposited OTE plates were removed from the reactor, dried and subsequently sintered at 300°C for 1 h. Two electrodes were also obtained by this method differing only on the relative contents of anatase and rutile.

{C} The TiO_2/OTE electrode obtained by the sol–gel method was prepared as follows: titanium tetraisopropoxide (284 g), diethanolamine (210 g) and ethanol (92 g) were mixed at ambient temperature in a nitrogen-filled glove box so as to avoid hydrolysis of the Ti(IV) compound. A solution of ethanol (4.6 g) and water (18 g) was then added to the stirred mixture and agitation continued for 1 h at ambient temperatures. This mixture was the dip-coating solution used to prepare the TiO_2/OTE plate by the sol–gel method [16,17]. The coated plate was dried at 50°C for 30 min in air and then heated at 400°C for 1 h to permit formation of a nanocrystalline TiO_2 thin film. The experimental operations of coating, drying and heating were repeated about 10 times to obtain a film of the desired thickness.

These three types of TiO_2/OTE plates were employed to examine the photodegradation of the DBS surfactant and BS. The anatase/rutile fraction $I_a/(I_a + I_r)$ was determined by XRD measurements from the intensities of the highest peaks (I_a = anatase, $2\theta = 25.28°$; I_r = rutile, $2\theta = 27.42°$) in the XRD patterns [18]. The overall features of the film surface and cross-sections of the TiO_2/OTE plates were examined by SEM microscopy. The constituents of the electrodes were analyzed by electron dispersive X-ray diffractometry (EDX).

2.2. Analytical measurements

The photoelectrochemical degradation device was described previously [12]. The DBS solution (0.1 mM, 50 ml; 5 μmol) was contained in a Pyrex glass photoreactor (headspace volume = 20.13 cm^3). The anode was a TiO_2/OTE plate, and the counter electrode (the cathode) was a Pt plate (20 × 20 mm^2); the reference electrode was a Ag/AgCl electrode connected to the assembly via a salt bridge. Applied voltages were obtained from a d.c. potentiostat. UV illumination (12.5 mW/cm^2 at λ_{max} 360 nm) was provided by a 75-W Hg lamp (Toshiba, $\lambda > 250$ nm). The potentials at the TiO_2 electrode were measured with an electrometer. The temporal evolution of CO_2 was assayed by gas chromatography using a Porapack Q column with helium as the carrier gas. A UV spectrophotometer was used to measure the extent of the breakup of the benzene ring during the course of the photodecomposition of DBS and BS.

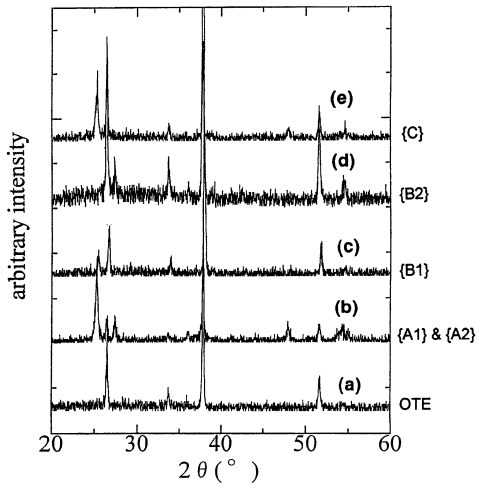

Fig. 1. XRD patterns of (a) an uncoated OTE plate, (b) TiO_2/OTE electrode prepared by the pasting method {A1 and A2}, (c) TiO_2/OTE electrode prepared by the pulsed laser deposition method ({B1}; $TiCl_4$:H_2:O_2 = 10:50:50 Torr), (d) same as (c) except that $TiCl_4$:H_2:O_2 = 10:100:25 Torr {B2}, and (e) TiO_2/OTE electrode prepared by the sol–gel method {C}.

3. Results and discussion

3.1. Crystalline type of TiO_2 loaded on OTE plates

The gas phase synthesis of TiO_2 by the pulsed laser photolysis of $TiCl_4$ in the presence of either H_2 and/or O_2 gases gave ultra small and pure particles of uniform size which resulted from dielectric gas breakdown. This procedure had the advantages of (1) light absorption efficiency, (2) no impurities were introduced into the TiO_2 particles, and (3) facile control of the formation ratio of anatase/rutile crystals was possible by altering the relative proportions of H_2, O_2 and $TiCl_4$.

The XRD pattern of an uncoated OTE plate displayed in Fig. 1(a) is that of the SnO_2 crystal layer making up the glass plate. The XRD patterns of the TiO_2/OTE plates prepared by the pasting {A1}, the pulsed laser deposition ({B1} $TiCl_4$:H_2:O_2 = 10:50:50 Torr, and {B2} $TiCl_4$:H_2:O_2 = 10:100:25 Torr), and the sol–gel methods are illustrated in the XRD patterns of Fig. 1(b), (c), (d) and (e), respectively. XRD diffraction lines for anatase and rutile are superposed onto those of the SnO_2 layer. The crystalline structures of TiO_2, the anatase/rutile ratios and the film thicknesses are summarized in Table 1. Most of the electrodes had a relatively high anatase content: {A}, 75%; {B1}, 86%; and {C}, 79%. By contrast, the {B2} electrode fabricated by the pulsed laser procedure was 100% TiO_2 rutile.

3.2. Surface features and cross-section of TiO_2/OTE plates

SEM photographs of the surfaces and cross-sections of the TiO_2 electrodes prepared by the three methods {A}, {B} and {C} are displayed in Fig. 2a, b and c, respectively. The pasted TiO_2/OTE electrode consists of aggregated TiO_2 particles (Fig. 2a; aggregate size ca. 100–200 nm) with the film surface displaying a rather open and somewhat uneven structure. By contrast, the surfaces of both the pulsed laser deposited TiO_2 films (Fig. 2b; anatase or rutile) showed relatively homogeneous morphologies (TiO_2 particle size: ca. 100 nm). The surface of the sol–gel TiO_2/OTE plate was moderately flat but with an open structure (Fig. 2c). Also displayed in Fig. 2a–c are the SEM film cross-sections. They show that the TiO_2 films are formed by lamination of the particles on the OTE plates. For all the electrodes examined, the SnO_2 layer was ca. 1.0 μm thick. Except for the

Table 1
Crystalline forms of the TiO_2/OTE electrodes and film thicknesses

Electrode[a]	Preparation procedure	Sintering temperature (°C)	Anatase/rutile ratio	Film thickness (μm)
{A1}	Paste (0.83 mg cm^{-2})	300	75/25	4.0–4.2
{B1}	Laser pulse (10:50:50)[b]	300	86/14	0.5
{B2}	Laser pulse (10:100:25)[b]	300	0/100	0.45–0.5
{C}	Sol–gel	400	79/21	0.75–0.8

[a] See text.
[b] $TiCl_4$:H_2:O_2 composition (Torr).

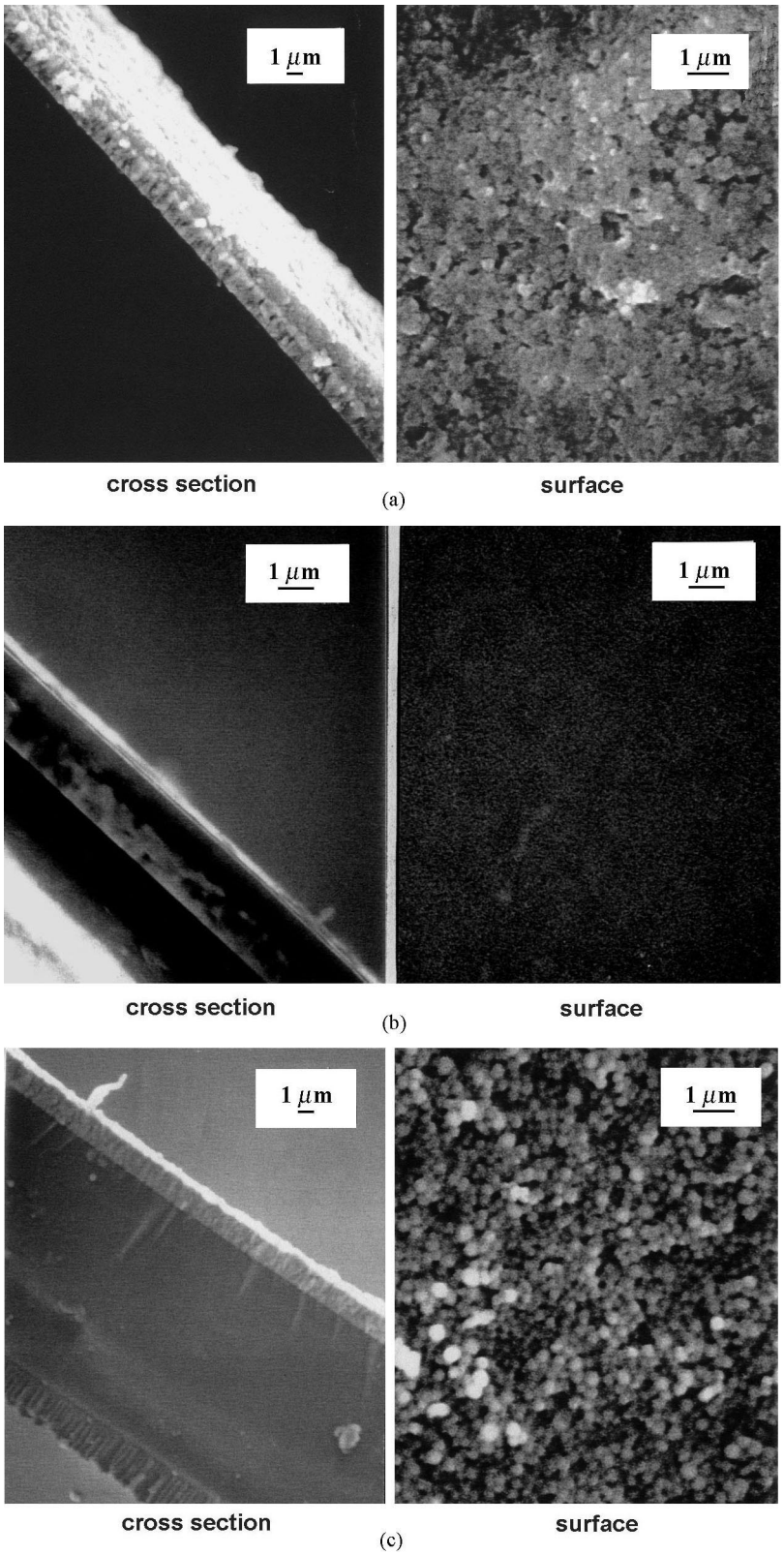

Fig. 2. SEM photographs displaying the surfaces and cross-section of electrodes prepared by (a) the pasting method, (b) the pulsed laser deposition method, and (c) the sol–gel technique.

{A1} electrode whose film thickness is about 4 μm, for all other TiO_2/OTE electrodes ({B1}, {B2}, and {C}) the film thickness ranged from 0.45 to 0.8 μm (Table 1).

3.3. Photoelectrochemical degradation of DBS and BS

The photodecompositions of DBS and BS (0.1 mM) on TiO_2/OTE electrodes in aqueous electrolyte solutions (NaCl 0.1 M) under an applied voltage (anodic +0.3 V bias vs. Ag/AgCl electrode) and in the absence of such bias are shown in Figs. 3–5. TiO_2/OTE electrodes made by pasting ({A2}, TiO_2, 0.41 mg/cm^2 and {A1}, 0.83 mg/cm^2), pulsed laser deposition (anatase and rutile TiO_2) and by the sol–gel method were used as photocatalysts for the photolysis. The disappearance of the aromatic ring in DBS and BS was detected by UV/Vis spectrophotometry. UV absorption attributable to the aromatic rings (at 224 nm for DBS, and 214 nm for BS) decreased under irradiation. Evolution of CO_2 gas from the DBS surfactant arises from a competitive mineralization between the aromatic ring and the alkyl chain.

Photodegradation of both DBS and BS in a photoelectrochemical system under an anodic applied bias clearly shows differences from that of a pure photochemical one on TiO_2/OTE plates (Figs. 3–5), differences that seem to depend on the type of electrode employed. For example, in

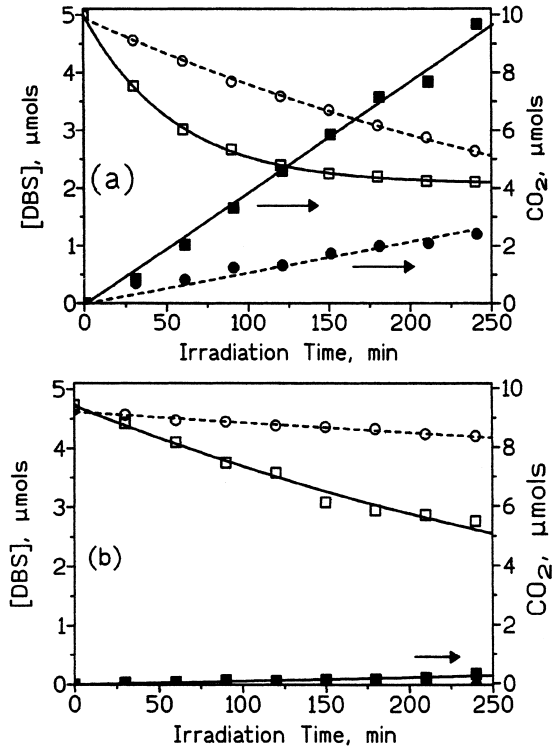

Fig. 3. Disappearance of the benzene ring and CO_2 evolution during the photodegradation of DBS (0.1 mM, 50 ml; 5 μmol) using a TiO_2/OTE electrode prepared by pulsed laser deposition: (a) anatase type {B1}; (b) rutile type {B2}. (○, ●): under no potential bias; (□, ■): at a constant bias of +0.3 V.

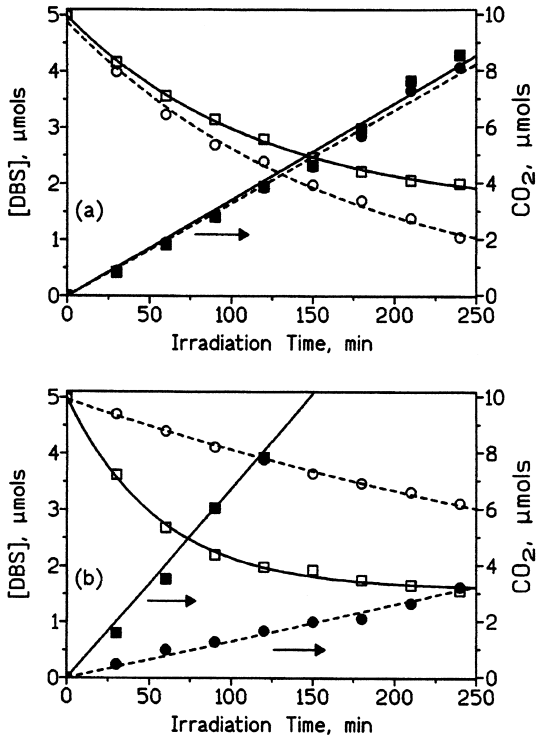

Fig. 4. Disappearance of the benzene ring and CO_2 evolution in the photodegradation of DBS (0.1 mM, 50 ml; 5 μmol) using a TiO_2/OTE electrode prepared by (a) pasting {A1}; and (b) by the sol–gel method {C}. (○, ●): under no potential bias; (□, ■): at a constant bias of +0.3 V.

the case where the {A1} TiO_2/OTE electrode was adopted, the photodegradation rates of both DBS (Fig. 4a) and BS (Fig. 5a) in the absence of applied bias were greater than those obtained under the constant bias of +0.3 V (Table 2). By contrast, when TiO_2/OTE electrodes prepared either by pulsed laser deposition ({B1}, Fig. 3a; {B2}, Fig. 3b) or by the sol–gel method ({C}, Fig. 4b) were employed, the photodegradation of DBS under the +0.3 V bias was constantly faster than was the case in the absence of bias. A similar behavior occurred when BS was photodegraded (Fig. 5b, c and Table 2). Hence except for the {A1} electrode, biasing the TiO_2/OTE electrodes always led to faster degradations of the two substrates, in one case by as much as an order of magnitude (DBS with the sol–gel electrode; Table 2). Of the three types of electrodes used, the sol–gel electrode {C} and the anatase {B1} electrode were most efficient overall when biased (compare the various results in Table 2 for k_{loss}). In the absence of any bias, however, the pasted TiO_2/OTE electrode was the more efficient electrode overall. It should also be noted that the little photoactivity displayed by the rutile TiO_2/OTE electrode {B2} increased substantially (sixfold) when the electrode was biased.

The largest percent loss of DBS and BS by photodegradation occurred for the pasted {A1} electrode in the absence of bias: 79% (loss of 3.9 μmol) and 89% (loss of 4.4 μmol), respectively, after 4 h of irradiation succeeded by the sol–gel

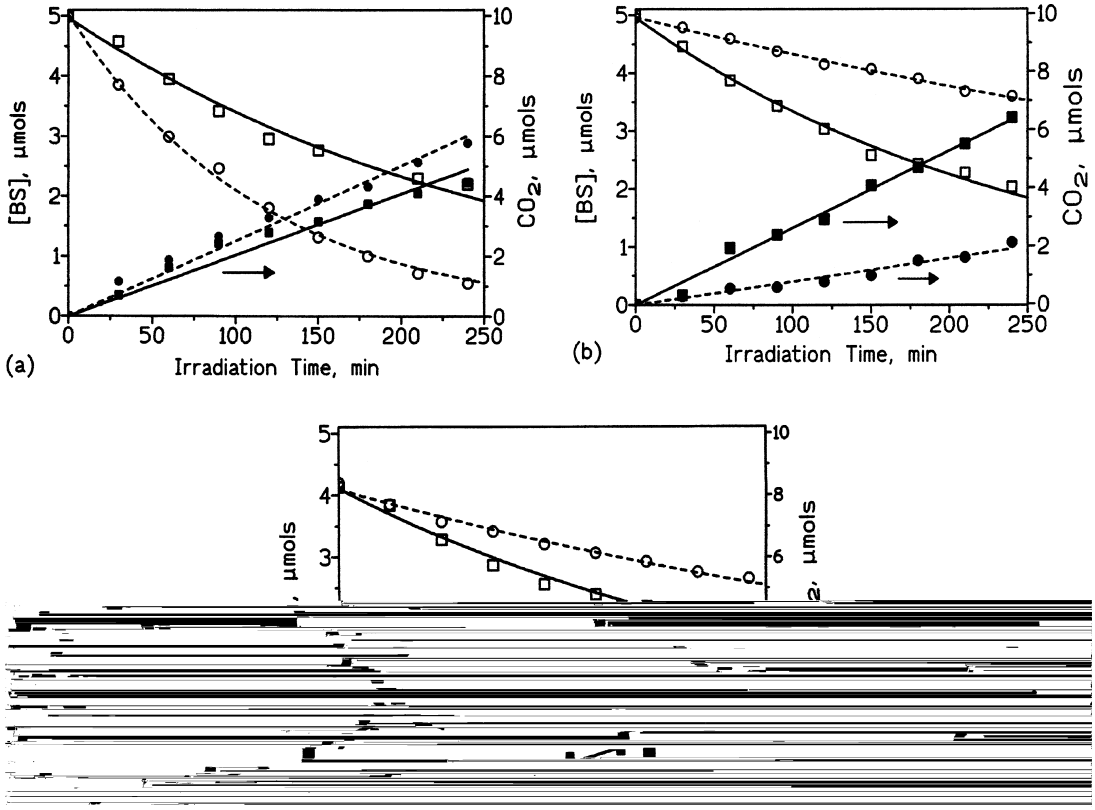

Fig. 5. Disappearance of the benzene ring and CO_2 evolution in the photodegradation of BS (0.1 mM, 50 ml; 5 μmol) using TiO_2/OTE electrodes prepared by (a) pasting {A1}; (b) the sol–gel method {C}; and (c) pulsed laser deposition (anatase, {B1}). (○, ●): under no potential bias; (□, ■): at a constant bias of +0.3 V.

Table 2
Kinetics of photodegradation of the DBS and BS surfactants ($C_0 = 5.0$ μmol) and of CO_2 evolution, and maximal photocurrents produced

	Anatase {B1}		Rutile {B2}		Paste {A1}		Sol–gel {C}	
Anodic bias	0 V	0.3 V	0 V	0.3 V	0 V	0.3 V	0 V	0.3 V
Dodecylbenzenesulfonate (*DBS*)								
k_{loss} (10^{-3} min^{-1})	2.63 ± 0.04	18.3 ± 0.4	0.40 ± 0.02	2.4 ± 0.1	6.2 ± 0.2	4.2 ± 0.2	1.98 ± 0.04	18.2 ± 1.0
$t_{1/2}$ (min)	263	38	1746	283	112	164	344	38
k_{CO_2} (10^{-3} μmol min^{-1})	10.8 ± 0.5	38.7 ± 0.6	0	1.25 ± 0.08	33.1 ± 0.5	34.3 ± 0.8	13.2 ± 0.3	67.6 ± 1.8
Percent loss of DBS[a] (μmol)	47 (2.4)	58 (2.9)	0 (0)	1.3 (0.4)	27 (8.1)	29 (8.6)	11 (3.3)	80 (24)
Percent CO_2 evolved[a,b] (μmol)	8 (2.4)	32 (9.7)	0 (0)	1.3 (0.4)	27 (8.1)	29 (8.6)	11 (3.3)	80 (24)
Maximal photocurrent[c] (mA)	–	2.31	–	–	–	0.49 (∼0.7)[d]	–	2.82
	Anatase {B1}		Paste {A1}		Sol–gel {C}			
	0 V	0.3 V	0 V	0.3 V	0 V	0.3 V		
Benzenesulfonate (*BS*)								
k_{loss} (10^{-3} min^{-1})	1.91 ± 0.08	3.51 ± 0.17	8.7 ± 0.2	3.8 ± 0.2	1.37 ± 0.04	3.95 ± 0.13		
$t_{1/2}$ (min)	363	197	79	183	505	176		
k_{CO_2} (10^{-3} μmol min^{-1})	10.1 ± 0.2	16.6 ± 0.5	25.1 ± 0.7	20.4 ± 0.8	8.2 ± 0.3	26.6 ± 0.5		
Percent loss of BS[a] (μmol)	37 (1.6)	54 (2.2)	89 (4.4)	56 (2.8)	27 (1.4)	59 (2.9)		
Percent CO_2 evolved[a] (μmol)	10 (2.4)	15 (3.8)	19 (5.8)	15 (4.5)	7 (2.2)	22 (6.5)		
Maximal photocurrent[c] (mA)	–	1.32	–	0.35 (∼0.7)[d]	–	2.05		

[a] After 4 h of irradiation.
[b] Assumed CO_2 is evolved from the break-up of the benzene ring in DBS.
[c] Within 1 h of irradiation.
[d] For the {A2} electrode (see text).

electrode at 68% (3.4 μmol) for DBS and 59% (2.9 μmol) for BS but under the applied bias. These losses, however, were not followed by a similar trend in the extent of CO_2 evolved for the same irradiation time. In fact, the largest quantity of carbon dioxide was produced for the sol–gel electrode {C}; ca. 80% or 24 μmol of CO_2 from DBS (Table 2). The latter represents approximately 7 carbon atoms of DBS that were converted to CO_2 which likely originates mostly from the aromatic ring and to a lesser extent from the aliphatic chain, since the latter is less easily oxidized by the surface $^{\bullet}OH$ radicals on the TiO_2 film surface than is the aromatic ring (note that addition of $^{\bullet}OH$ radicals to an aromatic ring is faster (e.g. $k_{OH} = 7.9 \times 10^9\,M^{-1}\,s^{-1}$ for benzene in aqueous media [19]) than is H atom abstraction from an aliphatic substrate (e.g. $k_{OH} = 1.4 \times 10^9\,M^{-1}\,s^{-1}$ for ethane also in aqueous media [20])). By contrast, for the same sol–gel electrode only 2 carbon atoms are converted to CO_2 from the degradation of the BS model compound under otherwise identical conditions. We cannot preclude differences in adsorption between DBS and BS on the TiO_2 film. Unfortunately, details of these differences cannot be described by the available data.

The results above and those summarized in Table 2 show that the TiO_2 crystalline type significantly affects the photodegradation kinetics; that is, electrodes that have a larger content of anatase are constantly more photoactive.

The temporal evolution of photocurrents in the photoelectrochemical decomposition of DBS and BS under the applied +0.3 V bias (vs. a Ag/AgCl reference electrode) using the pasted, laser-flashed and sol–gel TiO_2/OTE electrodes is illustrated in Fig. 6. The photocurrent obtained in the degradation of DBS was larger than in the degradation of BS for the same TiO_2/OTE working electrodes. The current decreased gradually with UV illumination time. The magnitude of the photocurrent varied directly with the decomposition rate. For example, the sol–gel TiO_2/OTE electrode yielding the greatest rate for DBS photoelectrolysis exhibited the maximum photocurrent, whereas the pasted electrode with the lowest rate gave the smallest current. It is curious, however, that although the anatase {B1} yielded kinetics similar to those of the sol–gel electrode {C}, the photocurrent produced was constantly lower for the {B1} electrode. No doubt the surface properties of the TiO_2 film that influence photodegradation must be different from those that affect electrical conduction between particles (see, e.g. Scheme 1).

In the absence of any applied voltage, photo-oxidation and photoreduction occur on UV-irradiated TiO_2 surfaces in the presence of suitable electron donors and acceptors, respectively. By the application of a constant bias of +0.3 V, oxidation of donors predominates because the nature of the photoelectrochemical cell is such that it causes the photogenerated electrons to migrate to the Pt counter electrode through the external circuit. This way, electron/hole recombination is efficiently hindered, and photo-oxidation of substrates on the TiO_2 surface is rendered more efficient. The surface conditions of the TiO_2 film, such as the surface area, TiO_2 particle size and crystalline structure also affect the photodegradative process. For example, using the pasted TiO_2/OTE electrode the rate was faster in the absence of bias because the surface area of the TiO_2 film with its cracks and roughness was significantly greater than for the other electrodes (see Fig. 2). However, under an applied voltage, the uniformity of the electrode film, the film thickness, and the contact of the film with the OTE plate, together with the overall UV transmittance of the film are all factors that are expected to influence the photodegradation kinetics and hence efficiency. Consistent with these notions, the degradation rate under the +0.3 V applied potential was greater for the thinner pasted TiO_2/OTE electrode (2.0 μm; 0.41 mg TiO_2 cm^{-2}) than for the corresponding thicker film electrode (4.0 μm; 0.83 mg TiO_2 cm^{-2}). Presumably, TiO_2 particles that are buried deep in the film are not likely to be irradiated owing to light absorption and scattering by the uppermost TiO_2 layers. Moreover, the photocurrent obtained from the thicker film is smaller because electrical conductivity in the thicker TiO_2 film is less efficient and the probability that the photogenerated electrons will reach the OTE plate is considerably lessened. Consequently, there may exist some appropriate optimal thickness of TiO_2 films to achieve rapid photodegradation under an applied voltage. Finally, both the photodegradation rate and the photocurrent must depend on the relative overall transmittance of the TiO_2/OTE electrode. The photocatalytic activity and the corresponding photocurrent of the sol–gel TiO_2/OTE electrode

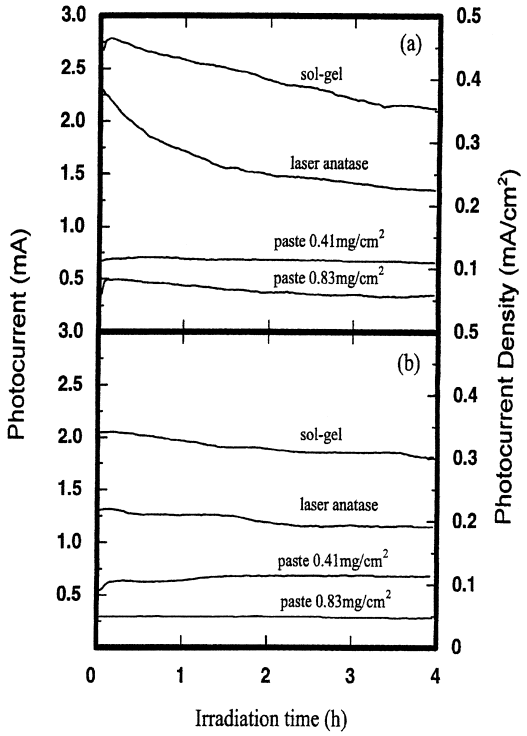

Fig. 6. Temporal photocurrents during the electrochemical photodegradation of (a) DBS, and (b) BS (0.1 mM, 50 ml; 5 μmol) at a constant bias of +0.3 V for various electrodes used.

are highest also because the electrical contact between the TiO_2 film and the OTE plate is appropriate for conduction.

4. Conclusions

The characteristics of TiO_2/OTE plates prepared by the laser pulse deposition method, the pasting method, and the sol–gel technique are different. The anionic surfactant DBS readily photodecomposed on the TiO_2/OTE plates within the irradiation conditions used and with or without an applied voltage. In the absence of bias, photodegradation was faster and correlates with the expected larger surface area of the TiO_2 film pasted on the OTE plate. TiO_2 thin films that are closely packed on the OTE plate facilitate the migration of photoelectrons to the OTE. The sol–gel electrode and the pulsed-laser electrode, in which the anatase content predominates, were more efficient in the degradation of the anionic surfactant DBS under the anodic bias. As expected, the pulsed-laser rutile TiO_2/OTE electrode was the least photoactive; however, application of the +0.3 V bias rendered this electrode six times more efficient. Before considering implementation of such thin film electrodes constructed by different procedures, however, it will be desirable to examine their efficiencies for a given polluted feed.

Acknowledgements

Financial support from the Frontier Research Center and from a Grants-in-Aid (No. 10640569) sponsored by the Japanese Ministry of Education is gratefully acknowledged. The work in Beijing is sponsored by the National Natural Science Foundation of China (No. 29677019 and No. 29725715) and the Foundation of the Chinese Academy of Sciences. Research in Montreal is supported by the Natural Sciences and Engineering Research Council of Canada. We thank Asahi Glass Co. for the kind gift of OTE glasses.

References

[1] S. Kato, F. Mashio, J. Jpn. Ind. Chem. (Jpn. Kogyo Kagahu Zasshi) 67 (1964) 1136.
[2] K. Vinodgopal, S. Hotchandani, P.V. Kamat, J. Phys. Chem. 97 (1993) 9040.
[3] K. Vinodgopal, U. Stafford, K.A. Gray, P.V. Kamat, J. Phys. Chem. 98 (1994) 6797.
[4] K. Vinodgopal, P.V. Kamat, Environ. Sci. Technol. 29 (1995) 841.
[5] K. Vinodgopal, P.V. Kamat, Solar Energy 38 (1995) 401.
[6] G. Marci, L. Palmisano, A. Sclafani, A.M. Venezia, R. Campostrini, G. Carturan, C. Martin, V. Rives, G. Solana, J. Chem. Soc., Faraday Trans. 92 (1996) 819.
[7] D.H. Kim, M.A. Anderson, Environ. Sci. Technol. 28 (1994) 479.
[8] D.H. Kim, M.A. Anderson, J. Photochem. Photobiol. A 94 (1996) 221.
[9] I. Moriguchi, H. Maeda, Y. Teraoka, S. Kagawa, J. Am. Chem. Soc. 117 (1995) 1139.
[10] I. Moriguchi, H. Maeda, Y. Teraoka, S. Kagawa, Chem. Mater. 9 (1997) 1050.
[11] Y. Maeda, M. Ichikawa, Y. Kudoh, Chem. Soc. Jpn. 3 (1997) 227.
[12] H. Hidaka, Y. Asai, J. Zhao, K. Nohara, N. Serpone, E. Pelizzetti, J. Phys. Chem. 99 (1995) 8244.
[13] H. Hidaka, H. Nagaoka, K. Nohara, T. Shimura, S. Horikoshi, J. Zhao, N. Serpone, J. Photochem. Photobiol. A 98 (1996) 73.
[14] H. Hidaka, T. Shimura, K. Ajisaka, S. Horikoshi, J. Zhao, N. Serpone, J. Photochem. Photobiol. A 109 (1997) 165.
[15] T. Oyama, Y. Iimura, T. Ishii, K. Takeuchi, J. Mater. Sci. Lett. 15 (1996) 594.
[16] K. Kato, Bull. Chem. Soc. Jpn. 65 (1992) 34.
[17] K. Kato, A. Tsuzuki, Y. Torii, H. Taoda, T. Kato, Y. Butsugan, J. Mater. Sci. 30 (1995) 837.
[18] K. Kato, A. Tsuzuki, H. Taoda, Y. Torii, T. Kato, Y. Butsugan, J. Mater. Sci. 29 (1994) 5911.
[19] L. Ashton, G.V. Buxton, C.R. Stuart, J. Chem. Soc., Faraday Trans. 91 (1995) 1631.
[20] N. Getoff, Appl. Radiat. Isot. 40 (1989) 585.